PHYSICAL REVIEW B **69**, 081201(R) (2004)

Influence of mobile dislocations on phase separation in binary alloys

Mikko Haataja[1] and François Léonard[2]
[1]*Princeton Materials Institute and Department of Mechanical and Aerospace Engineering, Princeton University, Princeton, New Jersey 08544, USA*
[2]*Sandia National Laboratories, Livermore, California 94551, USA*
(Received 25 November 2003; published 18 February 2004)

We introduce a continuum model to describe the phase separation of a binary alloy in the presence of mobile dislocations. The kinetics of the local composition and dislocation density are coupled through their elastic fields. We show both analytically and numerically that mobile dislocations modify the standard spinodal decomposition process, and lead to several regimes of growth. Depending on the dislocation mobility and observation time, the phase separation may be accelerated, decelerated, or unaffected by mobile dislocations. For any finite dislocation mobility, we show that the domain growth rate asymptotically becomes independent of the dislocation mobility, and is faster than the dislocation-free growth rate.

DOI: 10.1103/PhysRevB.69.081201 PACS number(s): 64.75.+g, 61.66.Dk, 61.72.−y, 81.05.Bx

Much effort has been devoted to studying the process of phase separation in alloys, motivated by a desire to better understand this industrially relevant problem, but also to explore the basic physics of nonequilibrium phenomena. Most theoretical and computational studies of phase separation in alloys have assumed perfect crystallinity of the material. However, real materials are far from this idealized situation, and usually contain a significant dislocation density.

Previous theoretical work on the coupling between phase separation and dislocations has already indicated the crucial role that dislocations play: enhancement of nucleation on dislocations,[1–5] hardening,[6,7] and acceleration of spinodal decomposition by discrete, immobile dislocations.[8] These studies have either focused on the time evolution of the composition in the presence of *static* dislocations, or dislocation motion in a static nonuniform composition. However, a theoretical description of the problem allowing for the coupled, simultaneous time evolution of the composition and dislocation fields is still lacking.

Experimental reports on thermomechanical treatment of phase separating alloys give an insight on the role of dislocations, as prior cold work increases the dislocation density. These experiments however have painted a conflicting picture. Cold work has been found to enhance[9,10] or reduce[11] phase separation, or even leave it unaffected.[12]

To address these issues, we present a model for a binary alloy phase separating by spinodal decomposition, in the presence of mobile dislocations. By coupling the composition and dislocations through their elastic fields, we show that mobile dislocations lead to several growth regimes. Asymptotically, the dislocations segregate to compositional interfaces and increase the interface tension. This increased interface tension causes an acceleration of the phase separation compared to the dislocation-free alloy. At intermediate times, the dislocations still segregate to interfaces, but their limited mobility creates a drag on the interfaces which decelerates the phase separation. At earlier times, there is another growth regime where the domain growth is unaffected by dislocations, due to a small dislocation density at the interfaces. Hence, as time proceeds there is a crossover unaffected → decelerated → accelerated, so that experimental measurements at different times may yield different conclusions on the role of dislocations.

We now introduce our theoretical approach. The binary alloy is described by a continuous composition $c(\mathbf{r})$ (relative to the average alloy composition) and a continuous Burger's vector density $\mathbf{b}(\mathbf{r})$.[13] The free energy is written as a sum of three terms, $\mathcal{F}=\mathcal{F}_c+\mathcal{F}_{\mathbf{b}}+\mathcal{F}_{coupl}$. Here $\mathcal{F}_c$ is the free energy due to the spatially varying composition, given by

$$\mathcal{F}_c=\int d\mathbf{r}\left[-\frac{a}{2}c^2+\frac{u}{4}c^4+\frac{\varepsilon^2}{2}|\nabla c|^2\right], \tag{1}$$

where $a=a_0(T_c-T)$, with T the temperature and T_c the critical temperature. a_0 and u are positive constants. The dislocation free energy $\mathcal{F}_{\mathbf{b}}$ is given by

$$\mathcal{F}_{\mathbf{b}}=\int d\mathbf{r}\left[\frac{\alpha}{2}|\mathbf{b}|^2+\frac{1}{2Y}(\nabla^2\chi_d)^2\right]. \tag{2}$$

The first term in this equation describes the local dislocation core energy. The second term accounts for the nonlocal elastic interactions (i.e., Peach-Koehler forces[14]) between the dislocations, where Y and χ_d denote the Young modulus and Airy stress function due to dislocation strain fields, respectively.[15] Under mechanical equilibrium conditions, the Airy stress function satisfies[16] $\nabla^4\chi_d=Y(\boldsymbol{\nabla}_x b_y-\boldsymbol{\nabla}_y b_x)$. Finally, the interaction between the composition and the dislocations arises due to the dependence of the lattice constant on the composition, $l(c)=l_0(1+\eta c)$, and its coupling to the local compression $\nabla^2\chi_d$,[8]

$$\mathcal{F}_{coupl}=\eta\int d\mathbf{r}c\nabla^2\chi_d. \tag{3}$$

The dynamics of the composition and dislocation density satisfy conservation laws and are given by

$$\frac{\partial c}{\partial t}=\Gamma\nabla^2\frac{\delta\mathcal{F}}{\delta c}, \tag{4}$$

$$\frac{\partial b_x}{\partial t}=(\Gamma_g\nabla_x^2+\Gamma_c\nabla_y^2)\frac{\delta\mathcal{F}}{\delta b_x}, \tag{5}$$

and

$$\frac{\partial b_y}{\partial t} = (\Gamma_c \nabla_x^2 + \Gamma_g \nabla_y^2) \frac{\delta \mathcal{F}}{\delta b_y}. \tag{6}$$

In these equations, Γ is the composition mobility while Γ_c and Γ_g are the dislocation mobilities in the climb and glide directions, respectively. Such evolution equations for the dislocation density $\mathbf{b}$ have been employed previously in the context of strain relaxation in heteroepitaxial films.[17]

Using the transformations $c \rightarrow (|a|/u)^{1/2} c$, $\mathbf{r} \rightarrow (\varepsilon^2/|a|)^{1/2}\mathbf{r}$, $t \rightarrow (\varepsilon^2/\Gamma|a|^2)t$, $\mathbf{b} \rightarrow (|a|^3/Y\varepsilon^2 u)^{1/2}\mathbf{b}$, and $\chi_d \rightarrow (Y\varepsilon^4/u)^{1/2}\chi_d$, we obtain the dimensionless dynamical equations

$$\frac{\partial c}{\partial t} = \nabla^2[\pm c + c^3 - \nabla^2 c + \gamma \nabla^2 \chi_d], \tag{7}$$

$$\frac{\partial b_x}{\partial t} = (m_g \nabla_x^2 + m_c \nabla_y^2) \times \left[\nabla_y \chi_d + \gamma \nabla_y \int d\mathbf{r}' G(\mathbf{r},\mathbf{r}') \nabla_{\mathbf{r}'}^2 c + \epsilon b_x \right], \tag{8}$$

a similar equation for $\partial_t b_y$ follows from Eq. (8) by replacing $b_x \rightarrow b_y$, $\nabla_y \rightarrow -\nabla_x$, and $\nabla_x \rightarrow -\nabla_y$. In the above, $\nabla_{\mathbf{r}}^4 G(\mathbf{r},\mathbf{r}') = \delta(\mathbf{r}-\mathbf{r}')$, and the top (bottom) sign in Eq. (7) is taken for $T > T_c$ ($T < T_c$). The new dimensionless parameters are $\gamma = \gamma Y^{1/2}/|a|^{1/2}$, $\epsilon = \alpha|a|/\varepsilon^2 Y$, and $m_{c,g} = \Gamma_{c,g}\varepsilon^2 Y/\Gamma|a|^2$.

We first discuss the equilibrium profile as a function of the coupling parameter γ. We take the negative sign in Eq. (7) corresponding to an alloy in the two-phase region of the phase diagram. To obtain the equilibrium profile for a given γ, we start from the known analytical solution $c(x,y) = \tanh(x/\sqrt{2})$ for the composition when $\gamma = 0$, and numerically integrate the coupled Eqs. (7) and (8) until a steady state is reached. (We use a finite difference Euler scheme on a uniform two-dimensional grid with periodic boundary conditions, grid spacing $\Delta x = \Delta y = 1.0$, and time step $\Delta t = 0.05$.) Figure 1 shows the composition and dislocation field b_y for different values of γ. The dislocations are localized at the interface, with a density that increases with γ. Since the dislocations have a uniform b_y component in the direction parallel to the interface and $b_x = 0$, the dislocation density at the interface is analogous to a line of discrete edge dislocations (misfit dislocations).

From the equilibrium profiles, we can extract the interface tension in the presence of dislocations, as shown in the inset of Fig. 1. Clearly, the interface tension is increased by the presence of dislocations. (Note that the total energy of the system, which scales with area, is reduced by the dislocations.) For the special case $\epsilon = 0$, the interface tension can be calculated analytically; the equilibrium composition profile is $c(x,y) = \sqrt{1+\gamma^2}\tanh(\sqrt{1+\gamma^2}x/\sqrt{2})$, giving an interface tension $\sigma(\gamma) = \sigma_0(1+\gamma^2)^{3/2}$. From the results of these *equilibrium* calculations, one would predict that dislocations accelerate the spinodal decomposition since they increase the interface tension.

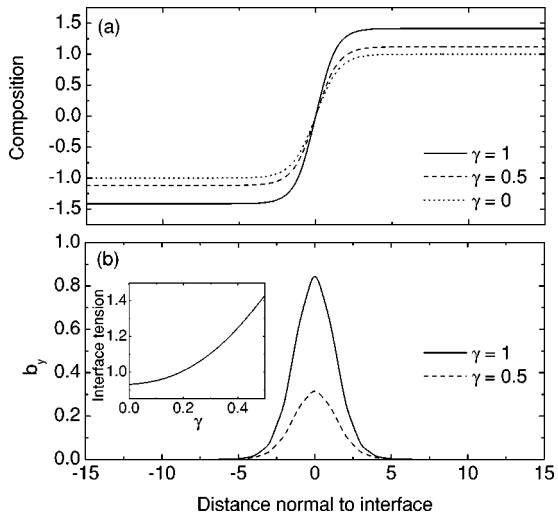

FIG. 1. Equilibrium profiles for (a) the composition field and (b) the dislocation field. The figures show half the cell in the system with periodic boundary conditions. The inset in (b) shows the interface tension calculated from the equilibrium profiles.

This expectation can be verified in the *fast dislocation limit* ($m_{c,g} \rightarrow \infty$) by performing a Lifshitz-Slyosov calculation of the growth of an isolated circular domain at late times.[18] For the case $\epsilon = 0$, the domain size $R(t)$ follows

$$R^3(t) = \frac{3\sigma(\gamma)}{[\Delta c(\gamma)]^2} t = \frac{3\sigma_0}{4}(1+\gamma^2)^{1/2} t, \tag{9}$$

where $\Delta c(\gamma)$ is the composition difference between the inside and outside of the circular domain. The domains thus coarsen faster in the presence of fast dislocations by a factor $(1+\gamma^2)^{1/2}$.

The above arguments suggest that, in the fast dislocation limit and at late times, spinodal decomposition is accelerated by dislocations. To verify these predictions, we simulated numerically the full time evolution of the phase separation. We integrated numerically the coupled set of dynamical equations, starting from a random initial profile for the composition and $\mathbf{b}(\mathbf{r}) = 0$. We used the parameters above, with $\gamma = 1$, $m_c = m_g \equiv m$, and simulated a 50-50 alloy.

We measured the average domain size as a function of time by mapping the composition field onto an Ising model and calculating the total length of interfaces $L(t)$ in the system; the average domain size is then $R(t) = A/L(t)$, where A is the total area of the system. Figure 2 shows the result of such a calculation averaged over four runs with different initial random fluctuations for systems of size 256×256. The average domain size for the larger mobility ($m = 5$, dashed line) increases faster than the dislocation-free case (solid line), and the well-known[18] $R(t) \sim t^{1/3}$ behavior of dislocation-free spinodal decomposition is maintained in the presence of fast mobile dislocations, as predicted by Eq. (9).

While these results clearly establish that, at late times and in the fast dislocation limit, spinodal decomposition is accelerated, Fig. 2 also shows that for smaller dislocation mobilities, the domain growth shows a nonmonotonic behavior, and a strong dependence on the dislocation mobility. (Different

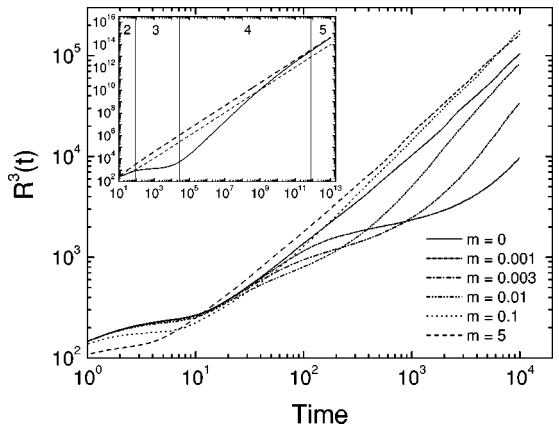

FIG. 2. Time dependence of the average domain size for different values of the dislocation mobility and for $\gamma=1$. The inset shows the predictions of Eq. (14) for $m=0.0025$ (solid line), highlighting regimes 2, 3, 4, and 5. The lower dashed line is for dislocation-free growth ($m=0$) and the upper dashed line is for fast dislocations ($m=5$). For clarity in the figure, we used $\gamma=4$ for this calculation.

materials have different dislocation mobilities, so varying the mobility in our model can be thought of as describing different materials.) Figure 3 shows snapshots of c and b_x at various times after the quench for dislocation mobilities $m_c=m_g=0.001$ for a system of size 128×128. As the images of Fig. 3 show, the dislocation density at the compositional interfaces varies significantly during the time evolution. This, coupled with a ''drag'' on the interfaces caused by the dislocations, leads to several regimes of growth, as we now discuss.

Immediately after the quench, the system is in the linear regime and fluctuations are amplified exponentially. We have calculated the maximum growth rate of fluctuations and found that it increases monotonically with increasing dislocation mobility. Hence, in this first regime, the phase separation is enhanced by mobile dislocations; this however only has the effect of decreasing the time the system spends in the linear regime.

The second growth regime corresponds to a situation of domain growth, with a very small dislocation density at the interfaces (top panels in Fig. 3); because of the small dislocation density at the interfaces, the average domain size follows closely that of the dislocation-free system.

The third regime occurs when the dislocation density at the interfaces becomes appreciable (middle panels in Fig. 3), and shows a deceleration of the domain growth compared to the dislocation-free system.

The behavior in these and subsequent regimes can be understood by performing an analysis of the domain growth for the coupled system. For simplicity, we set $\epsilon=0$, and take ∇_y of Eq. (8) minus ∇_x of the corresponding equation for b_y to obtain the two equations

$$\partial_t c=\nabla^2[-c+c^3-\nabla^2 c+\gamma\Theta] \tag{10}$$

and

$$\partial_t\Theta=-m(\Theta+\gamma c), \tag{11}$$

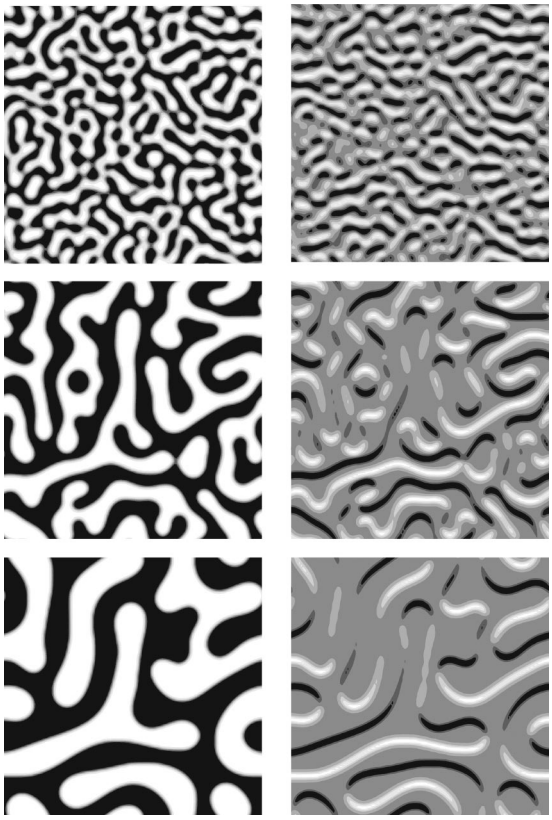

FIG. 3. Gray scale plots of the configurations as a function of time. The left panels show the composition c with black for $c=-1.5$ and white for $c=1.5$. The right panels show b_x, with black for $b_x=-0.9$ and white for $b_x=0.9$. Times from top to bottom are $t=20,\ 500,$ and $10\,000$.

where $\Theta=\nabla^2\chi_d$ and where we have set $m_c=m_g=m$. Explicitly solving for Θ and substituting the resulting expression in Eq. (10) yields an exact evolution equation for c which is nonlocal in time:

$$\partial_t c=\nabla^2\left[-c+c^3-\nabla^2 c-m\gamma^2\int_0^t c(t')e^{m(t'-t)}dt'\right]. \tag{12}$$

Upon writing $c(t')\approx c(t)+\partial_t c(t)(t'-t)$ and carrying out the integrals, we obtain the chemical potential

$$\mu=-c+c^3-\nabla^2 c-\gamma^2 c(1-e^{-mt}) -m\gamma^2\frac{\partial c}{\partial t}\left(\frac{te^{-mt}}{m}-\frac{1}{m^2}+\frac{e^{-mt}}{m^2}\right). \tag{13}$$

The above expression can again be readily analyzed for a circular domain of radius R'. Projection of Eq. (13) onto the interface yields the boundary condition

$$(\Delta\overline{c})\mu_{int}=-\frac{\overline{\sigma}}{R'}+\gamma^2 V\overline{\sigma}(te^{-mt}-1/m+e^{-mt}/m), \tag{14}$$

where V denotes the local speed of the interface, $\Delta\overline{c}=\Delta c_0\sqrt{1+\gamma^2(1-e^{-mt})}$ and $\overline{\sigma}=\sigma_0[1+\gamma^2(1-e^{-mt})]^{3/2}$. It

can be seen that mobile dislocations enhance the capillary term in μ_{int} which favors faster growth, and introduce a kinetic term which creates a drag on the interface; competition between these two factors gives rise to the nonmonotonic domain growth.

Solving the sharp interface problem $\nabla^2\mu=0$ and $\Delta cV=[\nabla\mu_{int}^{+}-\nabla\mu_{int}^{-}]\cdot\mathbf{n}$, where the susperscript $+$ $(-)$ denotes the gradient outside (inside) the circular domain evaluated at the interface and **n** denotes the interface normal, with the above boundary condition yields the following analytic expression for the coarsening rate:

$$\frac{dR}{dt}=\frac{\sigma_0\sqrt{1+\gamma^2(1-e^{-mt})}}{4R^2}\times\frac{1}{1-\dfrac{\gamma^2\sigma_0\sqrt{1+\gamma^2(1-e^{-mt})}(mte^{-mt}-1+e^{-mt})}{4mR}}. \tag{15}$$

Results of numerical integration of Eq. (15) are plotted in the inset of Fig. 2 for $m=0$, 0.0025, and 5, showing good qualitative agreement with our full numerical simulations (we used $\gamma=4$ in this calculation for clarity in the figure).

Since the velocity of interfaces decreases as time proceeds, the kinetic term in μ_{int} becomes less important at longer times, and there is a crossover to a regime of growth where the dislocation mobility is no longer a limiting factor. The average domain size in this regime increases rapidly. This corresponds to the fourth regime of growth (bottom panels in Fig. 3), and leads the system to the asymptotic regime.

The asymptotic regime is described by a fully saturated dislocation density at the interfaces, and slowly moving interfaces. We can estimate from Eq. (15) that the crossover to the asymptotic regime occurs when $t\gg m^{-1}$ and $R\gg m^{-1}$. In this regime, the dislocations increase the interface tension and accelerate the phase separation, as discussed for infinitely fast dislocations. This behavior is shown in Fig. 2, where at late times the average domain size for $m=5$ and $m=0.1$ converge to the same behavior.

To summarize, we have demonstrated both analytically and numerically that mobile dislocations modify the standard spinodal decomposition process, and lead to several new regimes of growth. Our work suggests a possible explanation for the conflicting experimental reports on the effects of cold work on phase separation[9–12] which have reported accelerated, decelerated, and unaffected domain growth. We hope that our work will stimulate more controlled experiments to elucidate the role of dislocations on phase separation.

F.L. acknowledges support from the Office of Basic Energy Sciences, Division of Materials Sciences, U.S. Department of Energy under Contract No. DE-AC04-94AL85000.

[1] C.C. Dolins, Acta Metall. **18**, 1209 (1970).
[2] J.W. Cahn, Acta Metall. **5**, 169 (1957).
[3] G. Sundar and J.J. Hoyt, J. Phys.: Condens. Matter **4**, 4359 (1992).
[4] S.Y. Hu and L.Q. Chen, Acta Mater. **49**, 463 (2001).
[5] S.Y. Hu and L.Q. Chen, Comput. Mater. Sci. **23**, 270 (2002).
[6] J.W. Cahn, Acta Metall. **11**, 1275 (1963).
[7] D. Rodney, Y. Le Bouar, and A. Finel, Acta Mater. **51**, 17 (2003).
[8] F. Léonard and R.C. Desai, Phys. Rev. B **58**, 8277 (1998).
[9] R.R. Bhat and P.P. Rao, Z. Metallkd. **75**, 237 (1994).
[10] J.T. Plewes, Metall. Trans. A **6A**, 537 (1975).
[11] F.T. Helmi and L. Zsoldos, Scr. Metall. **11**, 899 (1977).
[12] S. Spooner and B.G. Lefevre, Metall. Trans. A **11A**, 1085 (1975).
[13] In three dimensions, the dislocation density is described by a rank-two tensor (Ref. 16). In two dimensions, this tensor has only two nonzero components, which we denote as the two-component vector **b**.
[14] F. R. N. Nabarro, *Theory of Crystal Dislocations* (Dover, New York, 1967).
[15] The total Airy stress function is $\chi_{tot}=\chi_c+\chi_d$ where χ_c is due to the composition strain fields and χ_d is due to the dislocation strain fields. In writing Eqs. (1)–(3) we have already used the mechanical equilibrium condition to eliminate χ_c. This leads to local terms quadratic in c in the free energy, which simply renormalize T_c.
[16] L. Landau and E. M. Lifshitz, *Theory of Elasticity* (Pergamon, Oxford, 1986).
[17] M. Haataja, J. Müller, A.D. Rutenberg, and M. Grant, Phys. Rev. B **65**, 165414 (2002).
[18] J. D. Gunton, M. San Miguel, and P. S. Sahni, in *Phase Transitions and Critical Phenomena*, edited by C. Domb and J. L. Lebowitz (Academic, London, 1983), Vol. 8.